

This document was prepared in conjunction with work accomplished under Contract No. DE-DE-AC09-76SR00001 with the U.S. Department of Energy.

DISCLAIMER

This report was prepared as an account of work sponsored by an agency of the United States Government. Neither the United States Government nor any agency thereof, nor any of their employees, makes any warranty, express or implied, or assumes any legal liability or responsibility for the accuracy, completeness, or usefulness of any information, apparatus, product or process disclosed, or represents that its use would not infringe privately owned rights. Reference herein to any specific commercial product, process or service by trade name, trademark, manufacturer, or otherwise does not necessarily constitute or imply its endorsement, recommendation, or favoring by the United States Government or any agency thereof. The views and opinions of authors expressed herein do not necessarily state or reflect those of the United States Government or any agency thereof.

This report has been reproduced directly from the best available copy.

Available for sale to the public, in paper, from: U.S. Department of Commerce, National Technical Information Service, 5285 Port Royal Road, Springfield, VA 22161
phone: (800) 553-6847
fax: (703) 605-6900
email: orders@ntis.fedworld.gov
online ordering: <http://www.ntis.gov/support/index.html>

Available electronically at <http://www.osti.gov/bridge>

Available for a processing fee to U.S. Department of Energy and its contractors, in paper, from: U.S. Department of Energy, Office of Scientific and Technical Information, P.O. Box 62, Oak Ridge, TN 37831-0062
phone: (865)576-8401
fax: (865)576-5728
email: reports@adonis.osti.gov

TECHNICAL DIVISION
SAVANNAH RIVER LABORATORY

DPST-76-327

CC: R. E. Naylor, Wilm.
J. S. Neill
D. A. Ward, SRP
H. E. Wingo
C. H. Ice -
L. H. Meyer, SRL
J. R. Hilley
J. W. Wade
J. W. Stewart
M. M. Anderson
P. L. Roggenkamp
F. D. King
B. Crain
C. J. Temple
D. R. Muhlbaier
J. R. Taylor
J. P. Morin
J. D. Spencer
TIS File
Vital Records File

September 20, 1976

M E M O R A N D U M

TO: G. F. MERZ

FROM: S. D. HARRIS

TIS FILE
RECORD COPY

FLOW OF SLIGHTLY SUBCOOLED WATER AT
LOW PRESSURE THROUGH ORIFICES

INTRODUCTION

The rate of assembly flow decay following a postulated pump shaft break or power ramp accident has been shown experimentally to be determined by the large two-phase pressure loss through the endfitting (Ref. 1,2). Calculation of reactor transients by codes such as GRASS requires an analytical expression for flow vs. pressure drop for all stages of the flow transient. Single phase liquid flow through the endfitting is described by correlations given in assembly hydraulics manuals. Flow of steam through the endfitting is again a single phase problem to which information from SRL and Columbia tests can be applied.^(3,4) However, there are no data for the intermediate case, where coolant is subcooled upstream of the endfitting, but flashes to saturation (two-phase) conditions inside and downstream of the endfitting. This latter condition prevails during most of a postulated flow decay transient.

The purpose of this study is to provide experimental data for flow and pressure drop through endfitting orificing with low subcooling upstream, combined with saturated conditions downstream.

SUMMARY

Current SRL endfittings were modeled hydraulically by two sharp-edged single hole orifices in series. Orifice size and spacing were varied to simulate different numbers of shell and pressure plate holes. Flow and pressure drop were measured for various upstream subcoolings. Results were analyzed to obtain a correlation for the flow coefficient K , defined by

$$\Delta P = K \frac{G^2}{\rho g_c}$$

where:

ΔP = overall pressure drop,

G = mass flow rate M/L^2-T , and area of the upstream orifice is used

ρ = liquid density at upstream conditions, M/L^3

g_c = dimensional constant.

The flow coefficient can be correlated with upstream subcooling by a hyperbolic form

$$K = \frac{A}{(1 + T_{sub})^n} + B$$

where A , B , and n are empirical constants. B is the flow coefficient for the orifice at high subcooling (single phase). $(A + B)$ would be the orifice coefficient with saturated liquid (0° subcooling) upstream. T_{sub} is the difference between saturation temperature and actual coolant temperature between heated channel exit and endfitting. This difference is commonly called subcooling.

For a single orifice, the data are represented in a least squares sense by

$$K = \frac{22.22}{(1 + T_{sub})^{1.626}} + 1.212$$

where T_{sub} = upstream subcooling in $^\circ C$.

For two-orifices in series, the data is correlated by

$$K = \frac{9.1813}{(1 + T_{\text{sub}})^{1.636}} + 2.898$$

Although K was found to be a slight function of orifice spacing and of the ratio of diameters of upstream and downstream orifices, the error band in the data did not justify correlation of these variables. Figures 5 and 6 compare data and correlations.

These correlations reflect expected trends and magnitudes in full size assembly components, and can be used for testing assembly computer models. Steady state demand curves calculated for a Mark 16 are shown in Figure 10. Measurements of demand curves with an actual endfitting are currently in progress to check values for simple orifices, and appropriate refinements to the correlation made. Other correlating equations are currently being tried with the data. The goal is to find an accurate correlation that is also mathematically well behaved for transient calculations.

DISCUSSION

The endfitting insert shown in Figure 1 is placed in current SRP fuel assemblies to provide for continuous monitoring of coolant flow and outlet temperature by pressure and temperature sensors in the monitor pin nose. The endfitting insert has evolved with fuel assembly design from a simple orifice at the exit of a quatrefoil tube to the combination of orifice plates shown. The present design accommodates requirements for quadrant monitoring, variable assembly flow (zoning), and the limited span of the cantilevered flow transducers. It is satisfactory for monitoring single-phase liquid coolant flow.

The bottom fitting insert is composed of a:

- Venturi
- Quadrant divider
- Pressure plate
- Baffle plate
- Shell

The venturi near the top of the insert has a 2.75-inch-diameter throat to mix the subchannel effluents in each quadrant. A pressure plate with twenty-four 0.368 holes (number and size may vary) is directly below the venturi; the pressure plate increases the minimum pressure in the venturi and promotes mixing downstream. A mixed effluent sample flows from each quadrant through holes in the baffle plate, impinges on a monitor pin thermocouple, and exits through the monitor pin into the reactor tank. The remaining assembly flow discharges through holes in the shell above the baffle plate into

the reactor tank. The number of shell holes is varied to provide the desired ΔP transducer signal between the monitor pin nose and reactor tank bottom.

Flow in the endfitting when both liquid and vapor phases are present, as in an hypothesized power transient, will now be considered. The endfitting insert may be regarded as two orifices closely placed in series in a pipe. The pressure plate is the upstream orifice, and the shell hole/baffle plate combination is the downstream orifice. Simple orifices and the multiholed plates may both be characterized by flow cross sectional area to a first approximation. Complexities introduced by the venturi, quadrant divider, right-angle turn to exit the shell holes, and the tortuous path through the monitor pin are less significant than fluid phase change effects to flow transients discussed here.

For normal coolant flow and temperature, the water is single phase liquid throughout. A predictable overall pressure drop occurs across the pressure plate and the shell holes. Slightly downstream of both pressure plate and shell holes the fluid static pressure is further reduced because of increased velocity. In a simple orifice, this point of minimum pressure is called the vena contracta. Assembly hydraulics manuals list the minimum pressure as found by measurement, and the saturation temperature corresponding to this minimum pressure is a key factor in assigning assembly effluent temperature limits.

Now, suppose that assembly effluent temperature begins to rise rapidly, as in a power ramp type accident analysis. For constant mass flow rate, $G(\text{lbm}/\text{sec}\text{-ft}^2)$, liquid channel effluent temperature will approach saturation temperatures corresponding to static pressure at various points in the endfitting insert. When temperature reaches saturation temperature, some fraction of the liquid will "flash" to the vapor phase. The fraction that flashes to vapor depends on the enthalpy, or energy content, of the channel effluent liquid and the local static pressure. Flashing will usually occur first in the vena contracta of the shell holes because pressure here is the lowest anywhere in the assembly. However, this point is physically outside of the assembly, so that flashing here has no effect on assembly flow. As temperature increases, flashing will next begin at the minimum pressure point beneath the pressure plate, upstream of the shell holes and baffle plate. This flashing would cause an increase in pressure drop across the shell holes for constant mass flow. The pressure drop increases because the specific volume of the vapor-liquid mixture is greater than liquid alone. Fluid velocity in the shell holes is directly proportional to specific volume, and shell hole pressure drop is proportional to velocity squared. In the reactor system, overall pressure available to force coolant through assemblies is constant. Therefore, when shell hole pressure drop increases, the response of the assembly coolant system is to decrease mass flow slightly until pressure loss equals pressure available. In a power rise transient, this flow decrease produces an additional effluent temperature increase and even more vapor. Equilibrium of flow, power, and pressure drop is

possible until pressure loss exceeds pressure available. At that point the flow decay rate becomes self-enhancing and coolant flow reaches zero in the less than a second.

Safety analyses of reactor flow transients require that this flow decay time be calculated as precisely as possible. The zero flow point marks the beginning of rapid core material heating, and the release of significant quantities of steam into the moderator. This calculation requires a method of predicting the increased endfitting pressure drop with flashing and two phase flow.

Literature Review

Published data on two-phase pressure drop through orifices are applicable only: (1) in high pressure systems where changes in specific volume with pressure are moderate or negligible, or (2) where conditions are saturated upstream and downstream, with the assumption of thermodynamic equilibrium establishing conditions at all points along the fluid path through the orifice.

Flow transients in quatrefoil assemblies and early tubular assemblies such as the Mark V series were governed by friction pressure loss due to boiling in the annular channels. The channels were relatively longer and more narrow than present designs, and only a small fraction of total pressure drop occurred across the endfitting. Accordingly, experiments by Mirshak, (3) and at Columbia University, (4) were concerned with saturated flow upstream of the exit orificing.

Work that has been reported in the open literature for flashing flow pressure drop has limited application to SRP conditions. Recent Russian data reported in (5) describe system pressures exceeding 150 psia. SRP reactor pressures do not normally approach this pressure, and are only 28 psia at tank bottom. Henry, (6) and Henry and Fauske, (7) consider subcooled upstream conditions for short tubes over a wide range of pressures, but restrict application of their analysis for a sharp-edged orifice to conditions with saturated, two-phase mixtures upstream. Their analysis primarily concerns determination of the critical, or maximum, flow condition, for which choking is observed. Fitzsimmons data (8) combine high pressure with two-phase conditions both upstream and downstream of a single orifice.

Papers by Stuart and Yarnal, (9) and Kinderman and Wales, (10) describe experiments with identical orifices in series, discharging saturated water to atmosphere. Emphasis is on the "metastable" state (nonequilibrium) of the fluid between orifices, and in application of a dual orifice system as a steam trap for condensate removal. Data at subcooled upstream conditions from which a flow/pressure drop relationship could be derived are not given. Monroe (11) presents a correlation of data for one to four identical orifices in series with saturated water upstream. This report is perhaps the

closest antecedent to the present work. Results compared with Monroe's correlation are found to agree at zero subcooling (saturated water) upstream, but deviate at higher subcoolings. No information is given for nonidentical orifices or for effect of orifice spacing.

Test Equipment

The purpose of the experiments reported here was to provide pressure loss data for (reported) sharp edged orifices with low subcooling upstream of the orifice combined with low pressure downstream, simulating SRP reactor conditions.

The test loop is shown in Figure 2, and orifice test section details in Figure 3. Deionized water was preheated by DC resistance heating of a stainless steel tube 3.00" OD x 0.12" wall thickness with a 2.50" OD glass-reinforced plastic tube inside to form an annulus. From the heated section water flowed down through two feet of open steel tubing, 2.75" ID, to the orifice test section. From the test section the flow loop closed via a heat exchanger with temperature controlled bypass and a pump. An additional loop through a second heat exchanger and pump supplied colder water to the primary test loop downstream of the test section to quench steam before it reached the main heat exchanger and pump. This quenching system was found to be essential to maintain system hydraulic stability and to reduce pressure fluctuations at low subcoolings.

The orifice test section was constructed to permit changes in both orifice size and in spacing between orifices. The section of clear polycarbonate plastic tubing slips into flanges holding the orifices, sealed by O-rings. For tests with one orifice, the orifice was placed upstream of the clear section so that flashing could be observed. In tests with two orifices the intermediate space between orifices was visible. Orifice spacing was changed by lengthening the plastic section, and shortening the heated tubing upstream correspondingly. Table I lists the orifice sizes, combinations, and spacings tested, all with 2.75" ID tubing.

TABLE I

ORIFICE SIZES AND COMBINATIONS TESTED

<u>Test</u>	<u>Spacing</u>	<u>Orifice</u>	
		<u>Upstream</u>	<u>Downstream</u>
One Orifice	-	0.50 "	
		0.75 "	
		1.00 "	
		1.25 "	
Two Orifices	16 "	0.50 "	1.00 "
		0.75 "	0.75 "
		0.75 "	1.00 "
		0.75 "	1.25 "
		1.00 "	1.00 "
		1.00 "	1.25 "
	12 "	0.75 "	1.00 "
		1.00 "	1.00 "
		1.25 "	1.00 "
	6 "	0.75 "	1.00 "
		1.00 "	1.00 "

Orifices were the standard ASME sharp-edged design, as shown in the detail, Figure 3.

Instrumentation is shown symbolically in Figure 2. Temperatures were measured with iron-constantan thermocouples, referenced to 0°C, amplified and displayed on pen recorders. Signal conditioning amplifiers and chart recorders were calibrated daily with a Doric Model DS-350 Thermocouple Calibrator. Nominal ANSI limits of error assigned to iron-constantan thermocouple junctions are ±2°C. Although repeated calibration and close agreement with saturation line pressure-temperature values should assure error less than ±1°C, system noise under flashing conditions produced a pen trace whose width was as much as several degrees C. Temperatures were estimated by eye as the center of the band. Therefore, an error of ±2°C for temperature measurements is assigned.

Pressures upstream of the orifices and in the intermediate space were measured by static taps in the flanges, as shown in Figure 3. Downstream pressure was measured with a static pressure probe, positioned by trial to measure downstream pressure at full recovery in single phase conditions. Fluid pressure was fed to strain gage type pressure transducers, whose output signals were displayed on chart recorders. Transducers were calibrated daily against a laboratory Heise gage reserved only for calibration. System noise at low subcooling with flashing contributes more to measurement errors in the pressures than absolute error in instruments. The pressure measurement between orifices was noisiest, because the flow in that section is extremely turbulent and undeveloped. Pressure downstream of the second orifice was steady when conditions there were single phase, but noisy with flashing or quality flow. Pressure differences were obtained by subtraction of absolute pressures measured upstream and downstream. If $\pm 5\%$ error is assigned to individual pressure measurements, then combination of measurements to obtain ΔP could result in a probable error of $\pm 7\%$ if the individual errors are random with Gaussian distribution.

Mass flow was measured with a turbine-type in-line flow meter located on the discharge side of the pump (see Figure 2) where the water was always single phase. Output from this meter was recorded, and also used as the control signal for the flow control valve. The meter was calibrated with the laboratory volume rate calibration tank. Experimental error expected in flow measurement is $\pm 3\%$.

The test procedures for each orifice configuration were identical. Pressure and temperatures with no flow were recorded for calibration verification. Then, with cold water, a recording of flow and pressures for the range of selected flows was made to establish single phase characteristics. For single orifices this permitted a check of the orifice ΔP measured against expected ΔP from tables. The subcooling ($T - T_{sat}$) upstream of the orifice section was reduced by heating the water upstream in increments while maintaining mass flow constant. Pressure downstream of the orifices was established by the head tank level and system overpressure. Therefore, at low subcoolings the increased orifice ΔP caused upstream pressure to increase, with corresponding increase in upstream saturation temperature. As a result, the goal of zero subcooling was difficult to obtain with this type of apparatus. Incremental decreases in subcooling required larger and larger increments in input power. At high flow rates the heater power was sufficient to cause nucleate boiling and sometimes burnout (DNB) of the heater tube wall. The consequence of excessive nucleate boiling is that two phase, non-equilibrium fluid enters the upstream orifice rather than single phase liquid. Burnout of the heater tube wall is destructive. Data at exactly zero subcooling (saturated conditions) were not obtained at the higher flow rates. However, the system characteristic of continuously increasing upstream pressure with power did

ensure that zero subcooling was always approached from the sub-cooled side, and that saturated flow upstream with some small but finite quality did not occur.

Results

To illustrate overall results, pressure drop as a function of mass flow and upstream subcooling for two orifices in series is shown in Figure 4. The mass flow rate, G , is calculated based on the area of the upstream orifice. These curves were calculated using the empirical loss coefficient determined from all data. Note that at constant mass flow there is very little change in pressure drop between 40°C upstream subcooling (no flashing) and 5°C , where considerable vapor could be seen between orifices. At subcooling less than 5°C the change in pressure drop with subcooling is rapid. From this observation a correlation of the flow coefficient as a function of subcooling having the hyperbolic form

$$K = \frac{A}{(1 + T_{\text{sub}})} + B \quad (1)$$

would be expected to provide a suitable fit for the data. The independent variable is the liquid subcooling, T_{sub} , upstream of the pressure plate. The number B is the flow coefficient for the orifice at high subcooling. The quantity $(A + B)$ is the flow coefficient at zero subcooling. The flow coefficient K is defined by

$$\Delta P = K \frac{G^2}{\rho g_c} \quad (2)$$

where

ΔP = overall pressure drop, F/L^2

G = mass flow, $\text{M/L}^2\text{-T}$

ρ = liquid density at upstream conditions, M/L^3

g_c = dimensional constant, M-L/F-T^2

Data for a single orifice are shown in Figure 5. A least squares fit of all single orifice data is

$$K = \frac{22.22}{(1 + T_{\text{sub}})^{1.626}} + 1.212$$

A least squares method (HOKIE code) minimizing simultaneously the deviations in both K and T_{sub} coordinates was used because experimental error is expected in both quantities. Standard deviations between fitted curve and data are $\sigma_K = 0.378$ and $\sigma_{T_{\text{sub}}} = 0.433$. The ASME orifice coefficient C is defined by

$$G = C\sqrt{2g_c\rho\Delta P} \quad (3)$$

By comparing this expression to the defining equation for K in equation (2), the two coefficients are found to be related by

$$K = 0.5/C^2.$$

The ASME tables for sharp-edged orifices give $C = 0.628$ for pipe taps for water flow through an orifice with $d = 0.75$ inches in 2.75 inch pipe. The equivalent K is 1.27, which can be compared favorably with the fitted value of $B = 1.212$. The difference is less than one standard deviation in the K measurements.

Figure 6 shows data for two orifices in series. The least squares correlation of all two orifice data is

$$K = \frac{9.1813}{(1 + T_{\text{sub}})^{1.636}} + 2.898 \quad (4)$$

The standard deviations from the least squares fit are $\sigma_{T_{\text{sub}}} = 0.46$ and $\sigma_K = 1.3$.

Figure 7 shows the effect of orifice spacing on K , and Figure 8 the effect of varying the orifice diameters. Although K is certainly expected to vary with these parameters, the standard deviations of the data are so large that a distinction is not statistically justified.

Monroe⁽¹¹⁾ was able to correlate his data for N orifices in series with the following dimensional equation:

$$(N)^{0.75} \frac{G\mu}{(P_1-P_2)^2} = 36.4 \times 10^{10} \left[\frac{(P_1-P_2)T^2\rho}{\mu^2} \right]^{-1.193}$$

where

N = number of orifices in series

G = mass flow (lbsm/sec-ft²)

μ = upstream absolute viscosity (lbm/hr-ft)

(P_1-P_2) = total pressure drop (psi)

T = upstream absolute temperature (°R)

ρ = upstream density (lbm/ft³)

Monroe limited application of his correlation to: (1) equal diameter orifices (2) saturated upstream conditions, and (3) downstream pressure = 1 atm. A comparison of selected data from this study to Monroe's correlation is shown in Figure 9. Close agreement is shown for data with nearly zero subcooling upstream (<2°C), with deviations at higher subcoolings.

(E. S. Monroe is a Du Pont employee in the Engineering Department, Wilmington. In a telephone conversation, he advocated a flow coefficient approach to fitting the data instead of the arbitrary combination of variables given in his paper⁽¹¹⁾ as being simpler and probably more general.)

APPLICATIONS

Assembly critical effluent temperatures for reactor limit specification are currently based on measurements of assembly demand curves at Columbia University, with Mark VII-AL and Mark V-R mockups. The temperature corresponding to the minimum in a demand curve is taken to be the critical effluent temperature, where flow instability impends. Conservative adjustments are made in the calculation to compensate for the limited data base and for subsequent design changes. Correlations of the data presented, such as equation (4) can be used to calculate demand curves and the critical effluent temperatures without as much intuitive adjustment. Figure 10 is an example of demand curves for a Mark 16. (Figure 10 should not be used for limit calculations until equation (4) is verified by tests with an actual endfitting.)

Having an analytical expression for endfitting pressure drop also allows calculation of a flow decay transient. Currently, a flow decay time of 3 seconds is assigned in transient analyses based on average decay times measured in three Mark-VR tests at Columbia. A first order differential equation for momentum change of the coolant inside an assembly, incorporating Equation (4), can be written. Solution of this equation should model approximately a flow decay transient.

The essential assumptions in the derivation are:

- (1) One dimensional effects are dominant (average flow velocity, bulk friction factors can be used)
- (2) Coolant is single phase upstream of the pressure plate (hydraulics manual correlations can be used, with no nucleate boiling effects.)
- (3) Complex events in the endfitting are described by Equation (4).

Beginning with Newton's second law ($\Sigma F = ma$), the following equation for transient assembly flow is derived:

$$\frac{L}{g_c} \frac{dG}{dt} = (P_0 - P_3) + \frac{\rho g}{g_c} L - aG_1^n - K \frac{G^2}{\rho g_c}$$

1
2
3
4
5

where:

- 1 The "ma" term for the fluid in the coolant channels
- 2 Plenum to channel exit pressure drop
- 3 Static pressure head (L = assembly length)
- 4 Assembly channel pressure drop correlation derived from hydraulics manuals (G_1 = mass flow rate based on channel flow area)
- 5 The endfitting pressure drop, where K is obtained from Equation (4). (G = mass flow rate based on pressure plate orifice area. $G = G_1 * (\text{pressure plate orifice area/channel flow area})$).

The boundary condition on the solution would be the assembly power transient specified which continuously modifies the channel exit

subcooling (hence K and channel exit pressure, P_1). The equation is therefore non-linear in term 5, and numerical integration is difficult because the endfitting flow coefficient function K is very steep at low subcoolings. Figure 11 shows a trial solution of the equation, incorporating the correlation Equation (4). The solution does exhibit the long, slow flow decay caused by end fitting flashing. When $\Delta T_{\text{sub}} \rightarrow 0$, the slope of the flow decay becomes very steep and calculation was terminated. Comparison of this solution to flow transients measured in Ref. (2) suggests that the correlation derived from simple orifice data is too steep at low subcoolings. The general trend of the curve is correct. Measurements of the same type with an actual end fitting are being obtained with a mockup in A-station to refine the correlation.

SDH:vpb

REFERENCES

- (1) S. D. Harris and B. Crain, "Measurement of Flow Decay and Recovery Times with a Simple Assembly Model," DPST-73-422.
- (2) S. D. Harris, "Flow Instability Tests with Mark-16 Mockup in A-Station," DPST-75-528.
- (3) S. Mirshak, "Two-Phase Flow in Tubes with Outlet Orifices," (1955) (Secret).
- (4) Hoopes, J. W., "Flow of Steam-Water Mixtures in a Heated Annulus and Through Orifices," AICHE Journal, Vol. 3, No. 2, June 1957, pp. 268-275.
- (5) Keller, V.D., et al., "Research on Flow of Hot Water Through Orifices and Tubes," IVA-60 (Soviet-Swedish Symposium on Reactor Safety Problems), Studsvik, Sweden, March 1973.
- (6) Henry, R. E., "The Two-Phase Critical Discharge of Initially Saturated or Subcooled Liquid," Nucl. Sci. Eng., Vol. 41, 1970, pp. 336-342.
- (7) Henry, R. E., and Fauske, H. F., "The Two-Phase Critical Flow of One-Component Mixtures in Nozzles, Orifices, and Short Tube," ASME J. of Heat Transfer, Vol. 93C, May 1971, pp. 179-187.
- (8) Fitzsimmons, D. E., "Two-Phase Pressure Drop in Piping Components," HW-80970, Hanford Atomic Works, 1964.
- (9) Stuart, M. C., and Yarnall, D. R., "Fluid Flow Through Two Orifices in Series-III," Trans. ASME, Vol. 66, July 1944, pp. 387-397.
- (10) Kinderman, W. J., and Wales, E. W., "Fluid Flow Through Two Orifices in Series-III," Trans. ASME, Vol. 79, January 1957, pp. 183-190.
- (11) Monroe, E. S., "Flow of Saturated Boiler Water Through Knife-Edge Orifices in Series," Trans. ASME, Vol. 78, February 1956, pp. 373-377.

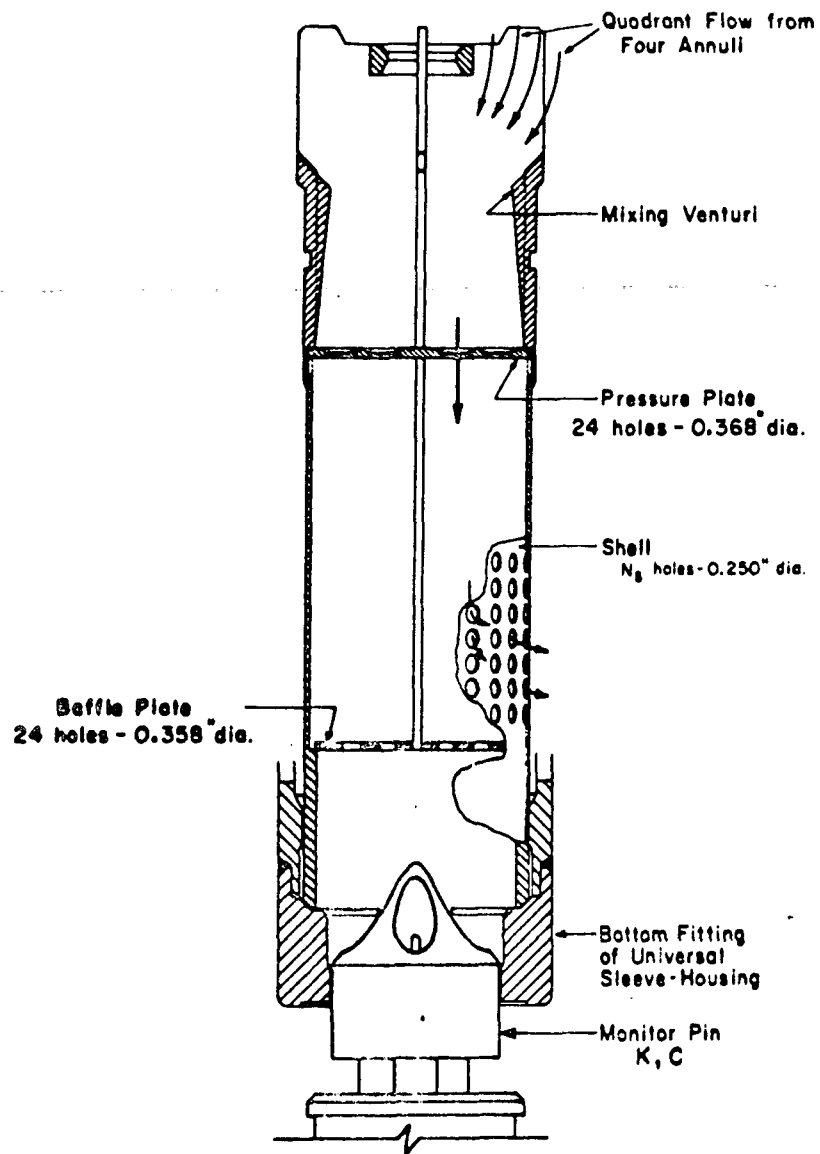


Figure 1. Typical fuel assembly endfitting insert

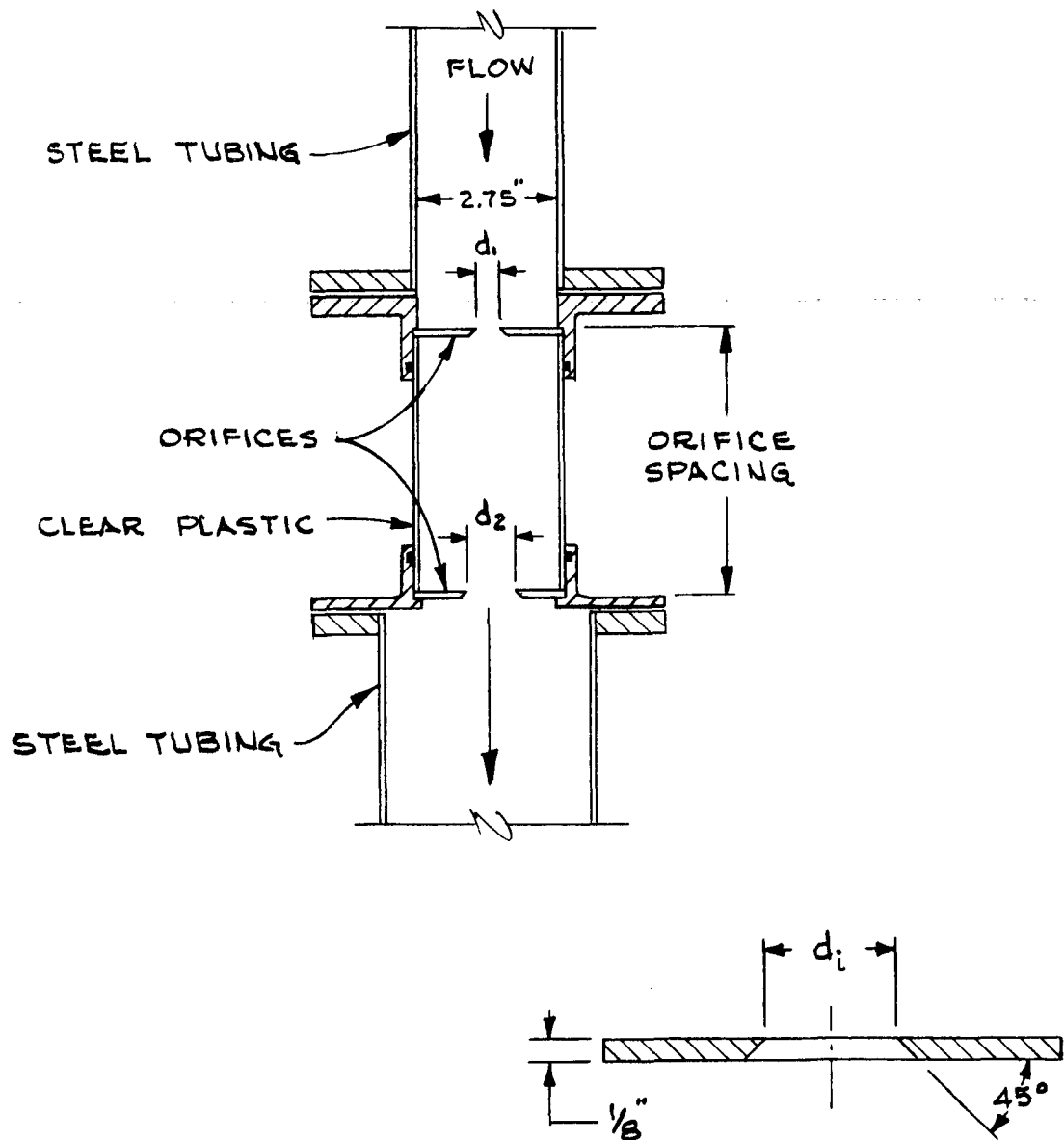


Figure 3. Test section schematic and orifice plate detail

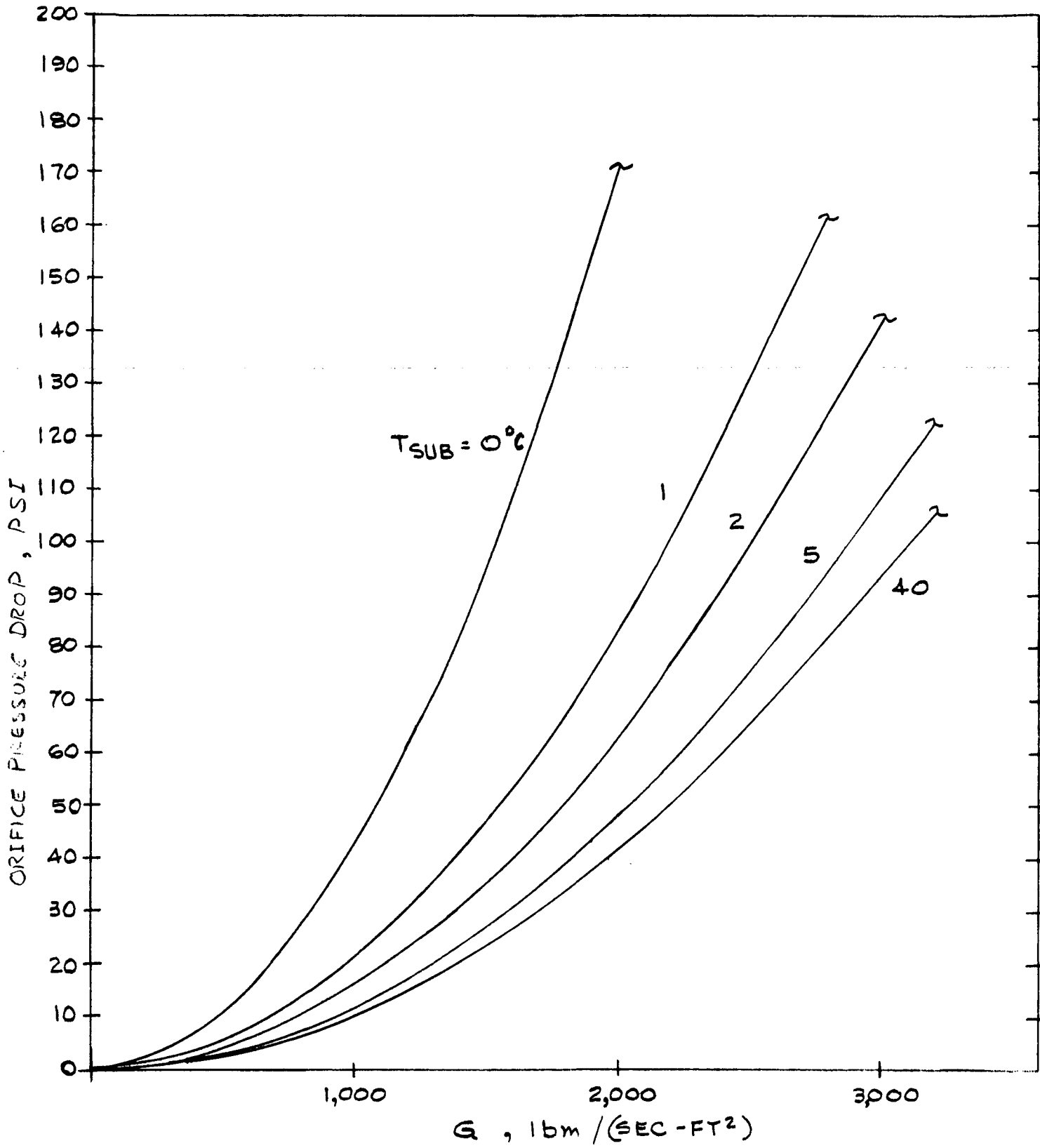
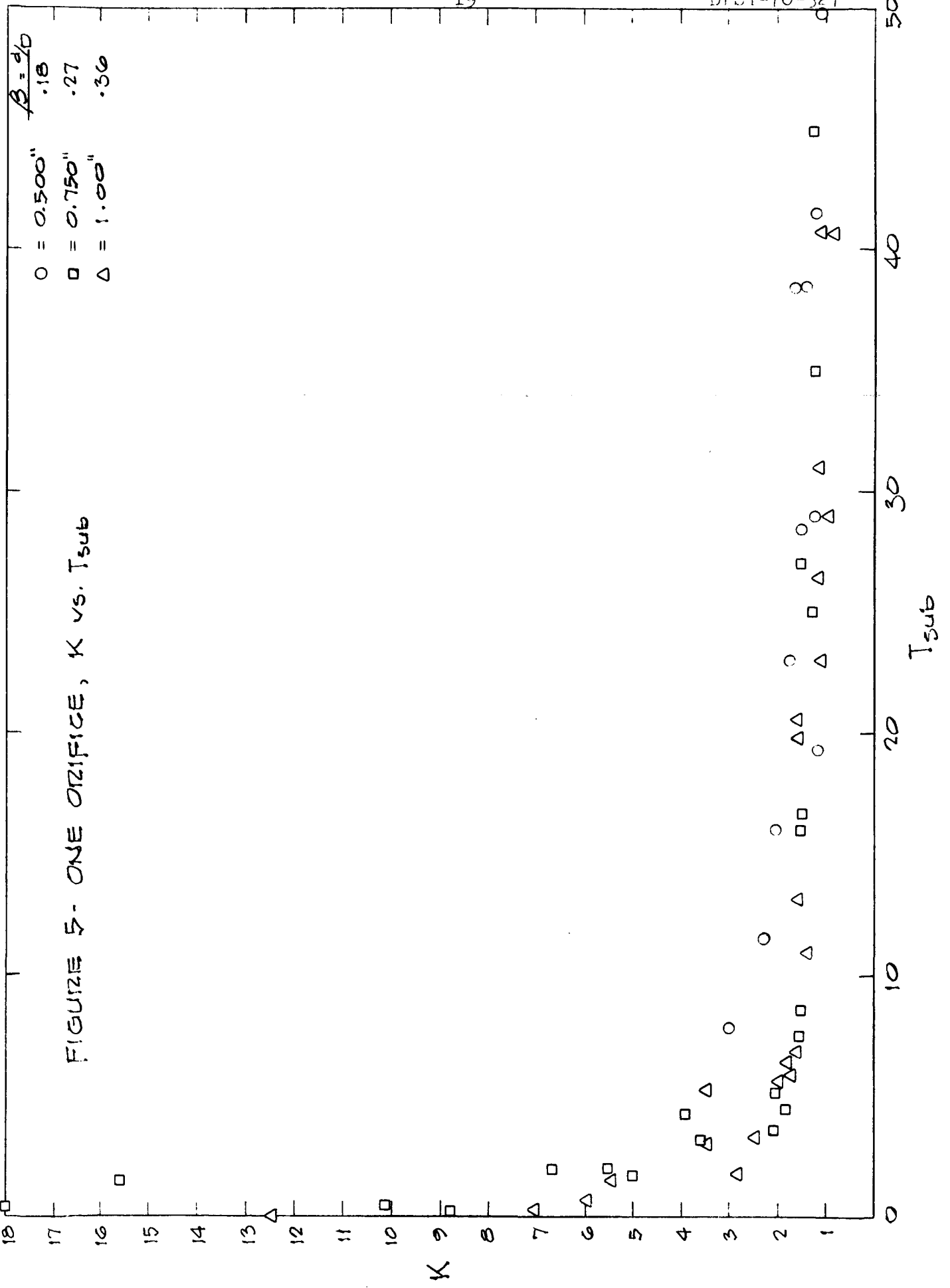


Figure 4. Typical pressure drop vs mass flow rate for two orifices at various subcoolings. Note that there is little effect for subcoolings $>5^{\circ}$.



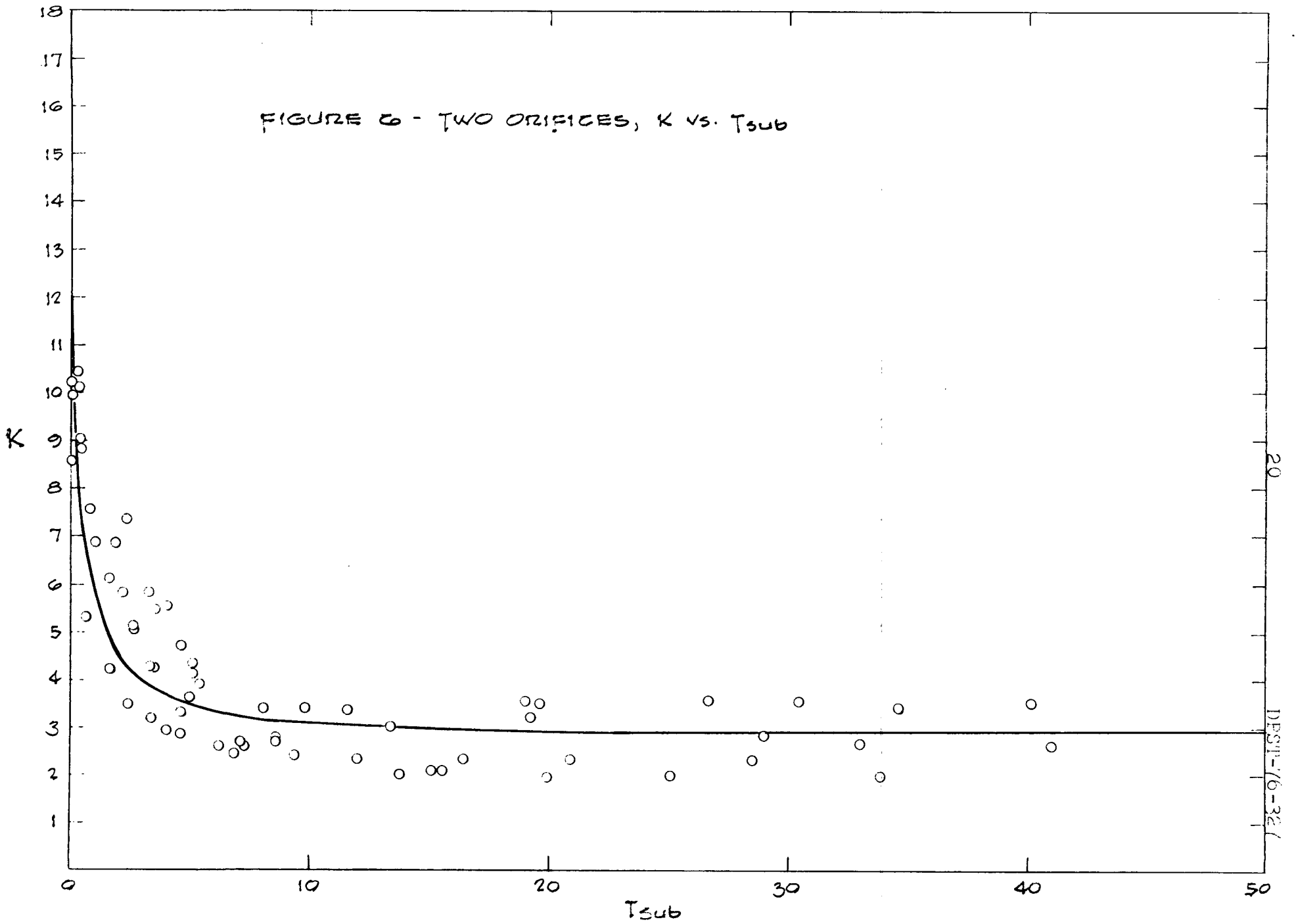


FIGURE 7 - TWO ORIFICES - EFFECT OF SEPARATION DISTANCE
(SCATTER MASKS EFFECT)

$d_1/d_2 = 1.0$

$L = 6''$

$12''$

$16''$

○

□

△

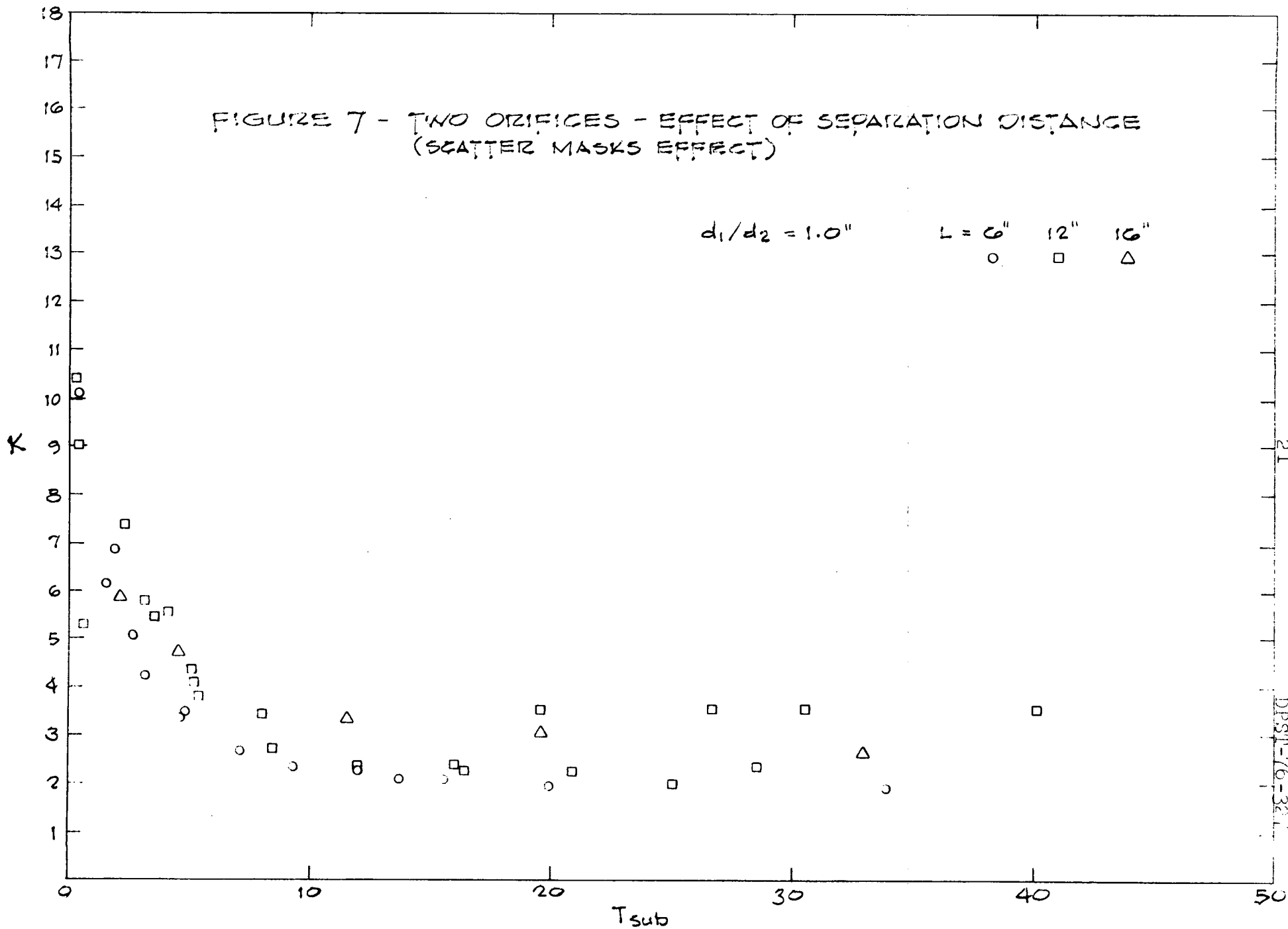


FIGURE 8 - EFFECT OF RELATIVE ORIFICE DIAMETERS FOR TWO ORIFICES (L = 6")

	d_1/d_2
—	.75"
- · - ·	1.00"
- - - -	1.25"

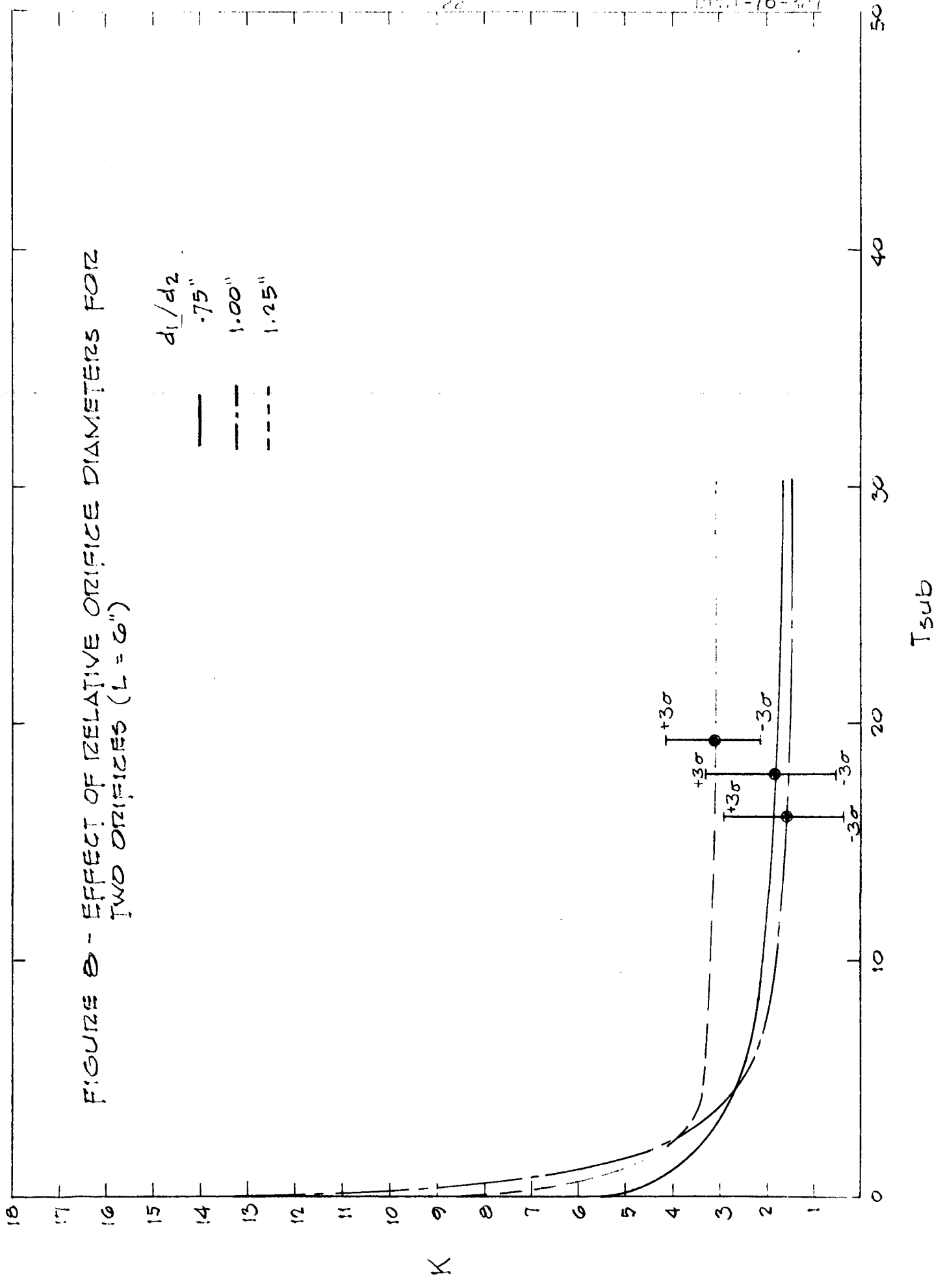
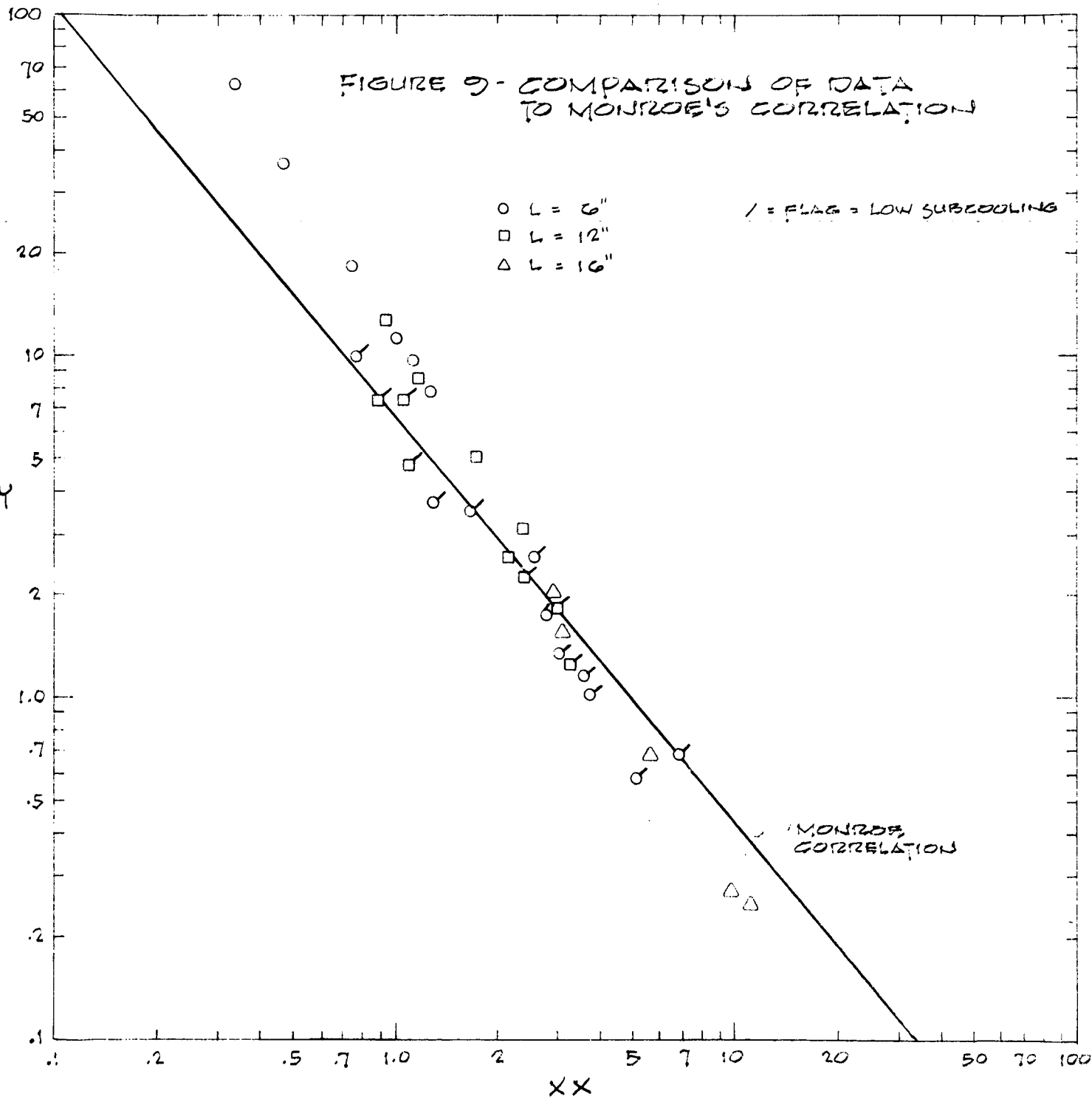


FIGURE 9 - COMPARISON OF DATA TO MONROE'S CORRELATION



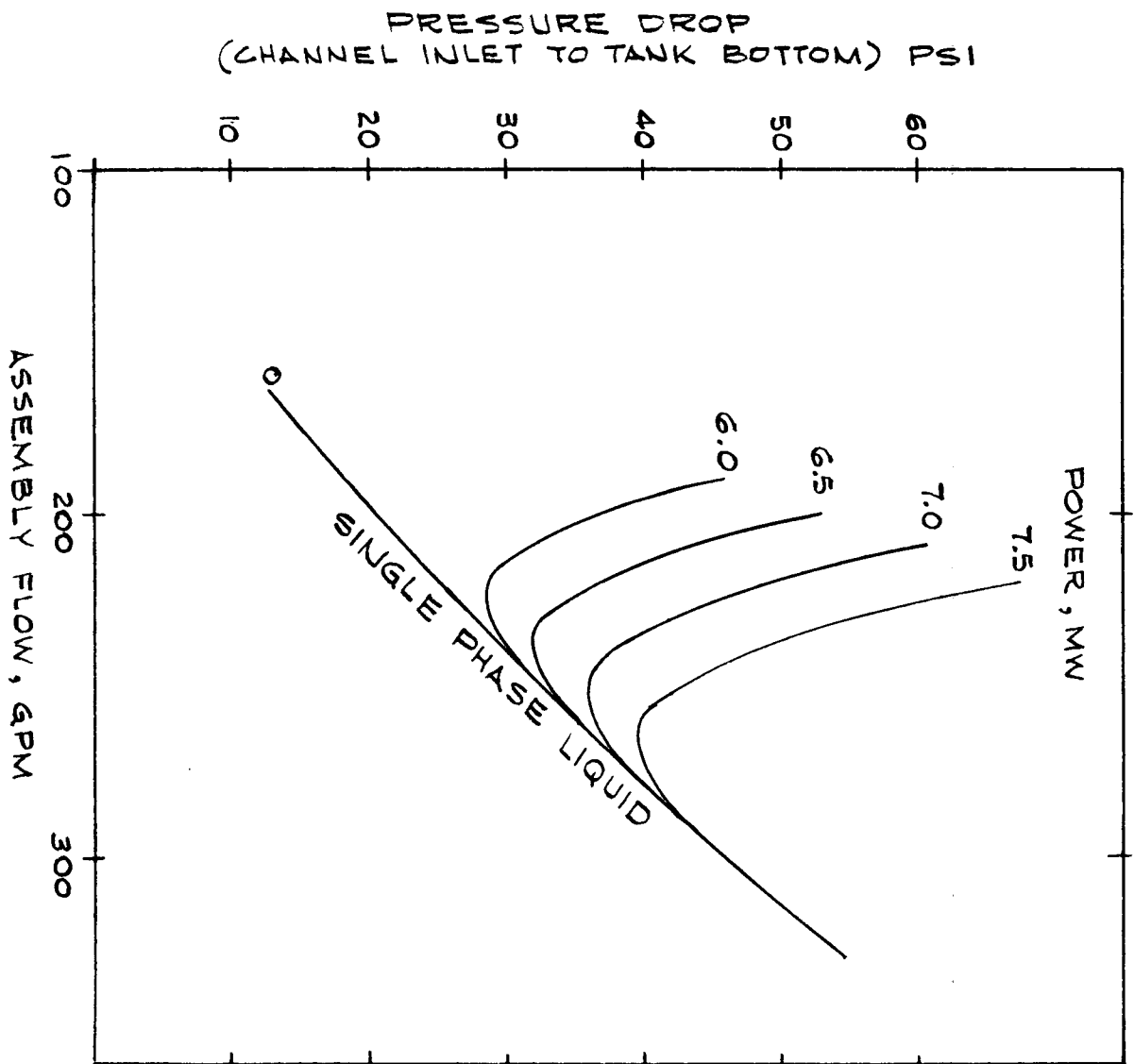
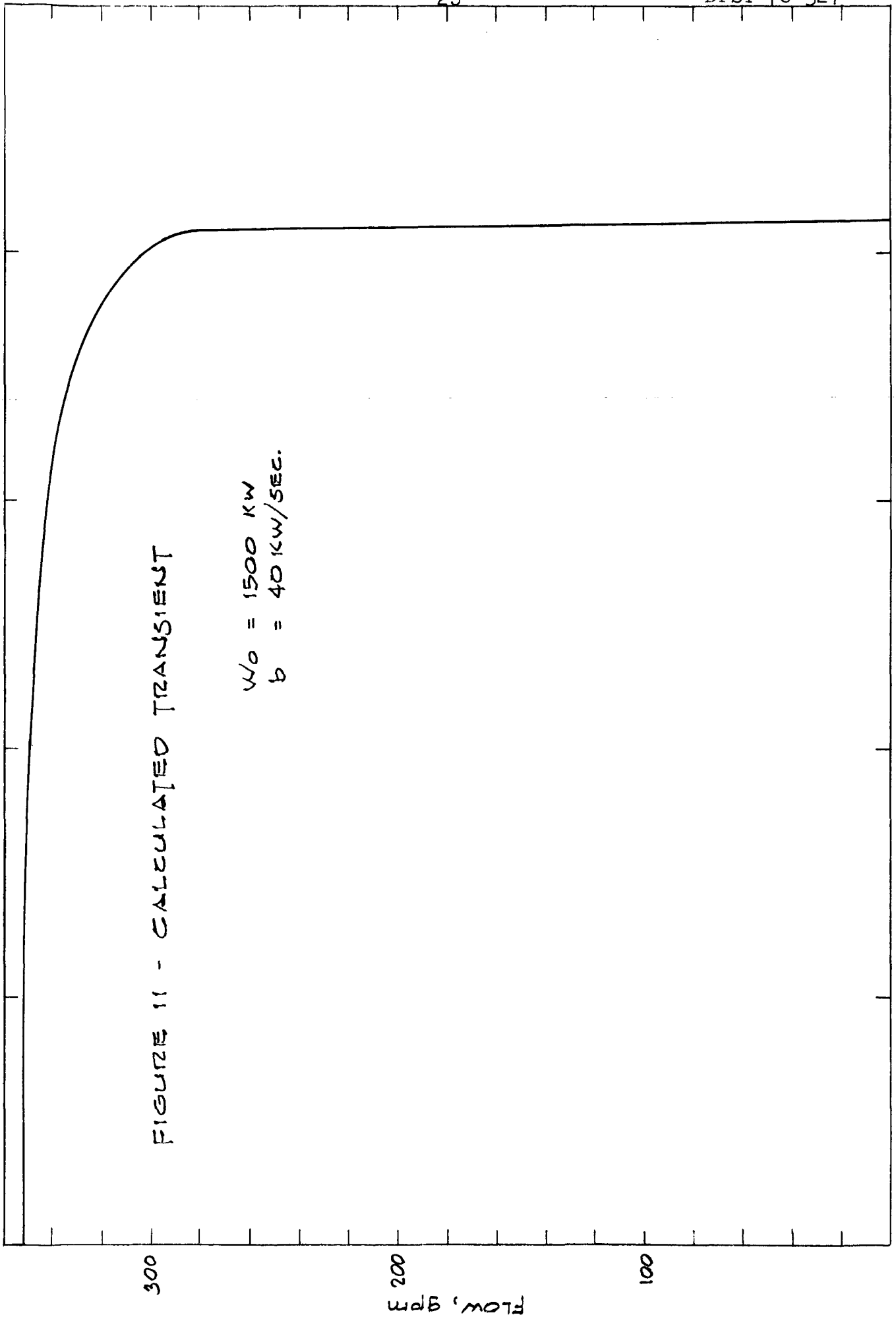


Figure 10. Demand curves for a Mk-16 calculated from correlations

FIGURE 11 - CALCULATED TRANSIENT

$W_0 = 1500 \text{ KW}$
 $b = 40 \text{ KW/SEC.}$



TIME, SEC.

FLOW, GPM

300

200

100

0

10

20

30

40